The Fine Structure of Singly Ionized Helium*†

WILLIS E. LAMB, JR. AND MIRIAM SKINNER‡

Columbia Radiation Laboratory, Columbia University, New York, New York

(Received January 26, 1950)

The displacement $2^2S_{\frac{1}{2}} - 2^2P_{\frac{1}{2}}$ in singly ionized helium has been determined to be $14,020 \pm 100$ mc/sec. The method is analogous to that employed for hydrogen by Lamb and Retherford, except that no beam of metastable ions is formed. Instead, helium atoms are bombarded by electrons of a few hundred volts energy. In about one percent of the ionizing collisions, the remaining atomic electron is excited to the metastable $2^2S_{\frac{1}{2}}$ state of the ion. When the bombardment region is illuminated with microwave radiation of the proper frequency, transitions to the $2^2P_{\frac{1}{2}}$ state are induced, and the ultraviolet photons emitted in the subsequent decay to the ground state $1^2S_{\frac{1}{2}}$ are detected by a suitable photoelectric detector. Background effects due to metastable atoms and radiation from HeI are reduced by the use of a collodion film filter. Our experimental value for the $2^2S_{\frac{1}{2}} - 2^2P_{\frac{1}{2}}$ level shift is about 1.4 percent higher than the present theoretical value.

1. INTRODUCTION

IN their experiment on the fine structure of hydrogen, Lamb and Retherford[1] showed that contrary to the predictions of the Dirac theory, states with the same principal quantum number, n, and the same total angular momentum quantum number, j, were not degenerate. In particular, they measured the energy difference between the $2^2S_{\frac{1}{2}}$ and the $2^2P_{\frac{1}{2}}$ states, using microwave techniques. In their first paper they reported a value of about 1000 mc/sec. for the frequency corresponding to this energy difference. After refining the measurement considerably, they obtained a value[2] of 1062 ± 5 mc/sec.

Shortly after the deviation from the Dirac theory had been established, Bethe[3] presented an explanation based on the interaction of the atomic electron with the radiation field. Using non-relativistic quantum electrodynamics, he showed that such an interaction would result in an upward shift of the energies of the $^2S_{\frac{1}{2}}$ states in a hydrogen-like atom, and a much smaller downward shift of the $^2P_{\frac{1}{2}}$ states, thus removing the degeneracy predicted by the Dirac theory. The numerical value obtained for this level shift was in qualitative agreement with the measured $2^2S_{\frac{1}{2}} - 2^2P_{\frac{1}{2}}$ energy difference.

Kroll and Lamb,[4] and French and Weisskopf[5] applied relativistic quantum mechanics to the calculation of the electromagnetic shift, and derived the following expression for the energy difference between the $n^2S_{\frac{1}{2}}$ and $n^2P_{\frac{1}{2}}$ levels of a hydrogen-like atom:

$$\Delta W_n = \frac{8\alpha^3}{3\pi} Ry \frac{Z^4}{n^3} \left[\log\frac{1}{\bar{\epsilon}} - \log 2 + \frac{23}{24} - \frac{1}{5} \right], \quad (1)$$

where α is the fine structure constant, Ry is the ionization energy of hydrogen, Z is the nuclear charge, n is the principal quantum number, and $\bar{\epsilon}$ is proportional to an average excitation energy of the atom. For hydrogen, using the latest[6] values of 135.549 mc/sec. for $\alpha^3 Ry/3\pi$ and 7.6915 for $\log 1/\bar{\epsilon}$, this theory gives 1051 mc/sec. for the level shift of the $2^2S_{\frac{1}{2}}$ state above the $2^2P_{\frac{1}{2}}$ state. There is therefore, to date, an 11 mc/sec. discrepancy between the theoretical and experimental values.

In order to subject the theory to further tests, it becomes of interest to examine the fine structure of singly ionized helium, a hydrogen-like atom of nuclear charge 2. In the experiment described below, microwave techniques were used to measure the energy difference between the $2^2S_{\frac{1}{2}}$ and $2^2P_{\frac{1}{2}}$ levels of singly ionized helium.

The theoretical value for the shift in He$^+$ can be found immediately from Eq. (1), noting that $Z = 2$, and that $\bar{\epsilon}(\text{He}^+) = 4\bar{\epsilon}(\text{H})$. The predicted level shift of the $2^2S_{\frac{1}{2}}$ state above the $2^2P_{\frac{1}{2}}$ state is then 13,820 mc/sec.

Several groups of spectroscopists have worked in the visible and ultraviolet regions on the fine structure of He$^+$. Paschen,[7] in 1916, investigated the fine structure of the $\lambda 4686$ line. His results constituted strong evidence

TABLE I. Measured fine structure in the He$^+$ spectrum.

	ΔW_n (in cm^{-1})	ΔW_2 (in 10^3 mc/sec.)
Mack and Austern[a]	$0.113 \pm 0.014(n=3)$	11.4 ± 1.4
Kopfermann and Paul[b]	$0.137 \pm 0.015(n=3)$	13.9 ± 1.5
Fowles[c]	$0.445 \pm 0.050(n=2)$	13.3 ± 1.5
Kopfermann[d]	$0.119 \pm 0.003(n=3)$	12.0 ± 0.3
Hirschberg and Mack[e]	$0.125 < \Delta W_3$ $< 0.134(n=3)$	$12.6 < \Delta W_2 < 13.6$

[a] J. E. Mack and N. Austern, Phys. Rev. **72**, 972 (1947).
[b] H. Kopfermann and W. Paul, Nature **162**, 33 (1948).
[c] G. R. Fowles, Phys. Rev. **74**, 219 (1948).
[d] Kopfermann, Krüger, and Öhlmann, Zeits. f. Physik **126**, 760 (1949).
[e] J. G. Hirschberg, Jr. and J. E. Mack, Phys. Rev. **77**, 745 (1950). We are indebted to Professor Mack for sending us these data.

[1] W. E. Lamb, Jr. and R. C. Retherford, Phys. Rev. **72**, 241 (1947).
[2] R. C. Retherford and W. E. Lamb, Jr., Phys. Rev. **75**, 1325 (1949).
[3] H. A. Bethe, Phys. Rev. **72**, 339 (1947).
[4] N. M. Kroll and W. E. Lamb, Jr., Phys. Rev. **75**, 388 (1949).
[5] J. B. French and V. F. Weisskopf, Phys. Rev. **75**, 1240 (1949).

[6] Bethe, Brown, and Stehn, Phys. Rev. **77**, 370 (1950). We are indebted to the authors for an opportunity to see their paper prior to publication. These authors conclude that $\bar{\epsilon}$ should not depend appreciably on the principal quantum number n. Unpublished calculations by B. S. Gourary confirm this expectation for $n=2$ and $n=3$, although the value for $n=1$ is somewhat different.

[7] F. Paschen, Ann. d. Physik **50**, 901 (1916).
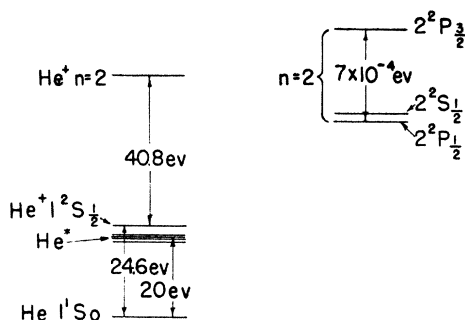
Fig. 1. Energy levels of He and He+.

Fig. 2. Cross-sectional diagram of the apparatus. The data reported here were taken with r-f radiation of about 1.6-cm wave-length, transmitted through the K-band guide C. This guide could be slipped out of the apparatus, however, and longer wave-lengths transmitted through the X-band guide L. J, a disk with a circular hole, defined the solid angle subtended by the detector plate at the excitation region. J was maintained at a positive potential with respect to D and E so that electrons ejected from J would not reach D.

of the essential correctness of the theoretical fine structure splitting of the energy levels of hydrogen-like atoms as developed by Sommerfeld, and later by Dirac. The results of the more recent work, pursued in the attempt to establish the anomalous fine structure of He+, are given in Table I. Fowles measured ΔW_2 by analysis of the ultraviolet $\lambda 1640$ line ($n=3\rightarrow n=2$). The others measured ΔW_3 by analysis of the visible $\lambda 4686$ line ($n=4\rightarrow n=3$). To facilitate comparison with the theoretical electromagnetic shift (and later with our result) the value in the last column represents in each case the corresponding shift of the $n=2$ level. This is obtained by assuming[6] a negligible change in $\bar{\epsilon}$ when n changes from 2 to 3, in which case, according to Eq. (1), $\Delta W_3/\Delta W_2$ is just 8/27. It is to be noted that the last two, more accurate, measurements are then low compared to the theoretical value of 13,820 mc/sec.

The experiment to be described below is capable of greater precision than those just mentioned for two reasons: the Doppler effect becomes negligible, and there is no complex of components to be analyzed.

2. METHOD

The possibility of applying microwave techniques to the measurement of the fine structure of He+ is suggested by the theoretical value of 13,820 mc/sec. for the shift of the $2^2S_{\frac{1}{2}}$ state above the $2^2P_{\frac{1}{2}}$ state. This corresponds to a wave-length of 2.2 cm, which is in an accessible range for microwave oscillators.

As in the case of hydrogen, the experimental method for ionized helium is based on the metastability of the $2^2S_{\frac{1}{2}}$ state. The energy levels of interest are shown in Fig. 1. An energy of 24.6 ev is required to remove one electron from the atom, and an additional 40.8 ev is required to excite the remaining electron to the group of states with $n=2$. The lifetime of the 2^2P states is

$$\tau = 1/A = 10^{-10} \text{ sec.,} \tag{2}$$

where A is the decay rate. (This is 16 times smaller than the lifetime of these states in hydrogen.) The $2^2S_{\frac{1}{2}}$ state, however, is metastable, the transition to the $1^2S_{\frac{1}{2}}$ ground state of the ion being forbidden by the selection rule $\Delta L = \pm 1$. The most probable decay method is double quantum emission, as shown for H by

Breit and Teller.[8] Making the appropriate changes in frequencies and matrix elements so as to use their calculations for He+, one finds that the expected lifetime of the $2^2S_{\frac{1}{2}}$ state is 2.2×10^{-3} sec., smaller by a factor of 64 than the lifetime of the metastable state of H.

The energy difference between the $2^2S_{\frac{1}{2}}$ and the $2^2P_{\frac{1}{2}}$ states can be measured in principle by obtaining a sufficient number of helium ions in the metastable $2^2S_{\frac{1}{2}}$ state (by electron bombardment of normal helium atoms), irradiating these with microwave radiation of the correct frequency in order to induce the transition to the $2^2P_{\frac{1}{2}}$ state and then, in some manner, detecting the decrease in the population of the $2^2S_{\frac{1}{2}}$ state.

The main difference between the work on hydrogen and that on singly ionized helium lies in the method of detection. In the hydrogen experiment, a beam of metastable atoms falls on a metal target and ejects electrons. The decrease in the population of the $2^2S_{\frac{1}{2}}$ state is inferred from the reduction in the electron current. Unfortunately, this detection method is not suitable in the case of He+. Although it is known that ions can eject electrons from metals, the relative ejection efficiencies of metastable and non-metastable ions are not known. Since, as we shall see below (Appendix II, Eq. (32)), the number of metastable ions produced by electron bombardment of normal helium atoms is about 1 percent of the number of non-metastable ions formed, large background currents would be unavoidable using this method of detection.

Because of this difficulty a photoelectric method of detection was adopted for the work with ionized

---

[8] G. Breit and E. Teller, Astrophys. J. **91**, 215 (1940).

helium. If a transition is induced from the $2^2S_{\frac{1}{2}}$ state to the $2^2P_{\frac{1}{2}}$ state, the ion then decays in 10^{-10} sec. to the ion ground state with the emission of a 41-ev photon. The photoelectric current produced by these photons striking a metal plate was used as a measure of the number of induced transitions. We shall refer to such induced transitions as r-f "quenching" of the metastable ions.

A cross-sectional diagram of the apparatus is shown in Fig. 2. A and B are pole pieces of a magnet. C is a wave guide. G is a hot filament maintained at a negative potential, so that electrons of a few hundred volts energy stream across the wave guide into the opposite pole piece and are collected on a metal plate at H. In contrast to the work with hydrogen, no attempt is made to form a beam of atoms in the $2^2S_{\frac{1}{2}}$ state. Instead, helium atoms circulate freely through the apparatus with thermal velocities. Some of the atoms in the bombardment region are excited or ionized, and a very small fraction of them are left in the $2^2S_{\frac{1}{2}}$ and 2^2P states of the ion. Those ions in the 2^2P states decay immediately to the $1^2S_{\frac{1}{2}}$ state with the emission of 41-ev photons. Those in the $2^2S_{\frac{1}{2}}$ state remain there until they diffuse out of the region and strike a wall or come into the presence of some other perturbing field which will cause them to decay. If, however, r-f of the proper frequency is introduced into the wave guide, the transition from the $2^2S_{\frac{1}{2}}$ state to the $2^2P_{\frac{1}{2}}$ state is induced, and the resultant $2^2P_{\frac{1}{2}}$ state decays to the ground state with the emission of an additional 41-ev photon. The photons are detected with a photoelectric detector which consists simply of a copper plate D and an electron collector E. The current from D to E is measured with an electrometer tube and a sensitive galvanometer.

The experiment is carried out in the presence of a magnetic field. One advantage derived from this is that charged particles cannot reach the detector. The main reason for the use of the magnetic field, however, arises from the difficulty of taking data by the direct method of varying the oscillator frequency. The $2^2P_{\frac{1}{2}}$ state has a natural width $A/2\pi = 1600$ mc/sec. Thus, in order to obtain a resonance curve by varying the frequency, one would require either a single oscillator tunable over a range of about 3000 mc/sec., centered at a frequency in the vicinity of 14,000 mc/sec. or a set of ten or twelve fixed frequency oscillators covering this range. In either case the practical difficulties are very great, owing to the wide range of frequencies involved, and to the requirement that the power be the same for all the measurements. In the presence of a magnetic field, it is possible to work at a fixed oscillator frequency and vary the field strength to obtain a resonance for one of the Zeeman component transitions, from which one can then easily obtain the zero magnetic field energy shift. In this case one has considerable latitude in the choice of the fixed oscillator frequency (limited only by the maximum magnetic field available and by the desirability of working in a region isolated from neighboring

Zeeman transitions), and the variation of the magnetic field over a wide range involves no problems comparable to those which one would encounter in varying the frequency.

3. ZEEMAN EFFECT

In the presence of a magnetic field, the $2^2S_{\frac{1}{2}}$ state and the $2^2P_{\frac{1}{2}}$ state are each split into two components (see Fig. 3). Transitions are possible between each of the components of the S state and each of the components of the P state. The transition frequencies as a function of the magnetic field are shown in Fig. 4. The significant data of this experiment were obtained by working with the upper (ad) transition,

$$2^2S_{\frac{1}{2}}(m=+\tfrac{1}{2})\rightarrow 2^2P_{\frac{1}{2}}(m=-\tfrac{1}{2}).$$

If the magnetic field is sufficiently weak, the energy of a given state is a linear function of the field strength, given by the expression

$$E=E_0+mg\mu_0 H, \qquad (3)$$

where μ_0 is the Bohr magneton, m is the magnetic quantum number, and g is the Landé g-factor. For small magnetic fields, the resonance energy for the (ad) transition is also a linear function of H, given in frequency units by

$$\nu_r = \nu_0 + (4/3)\mu_0 H/h = \nu_0 + aH, \qquad (4)$$

where

$$a = 1.866 \text{ mc/sec. per gauss.} \qquad (5)$$

In strong magnetic fields, the spin and orbital angular momentum vectors are decoupled, and Eqs. (3) and (4) no longer hold. For the magnetic fields used in this experiment (up to 4000 gauss) there is sufficient decoupling to require only a small correction to Eq. (4),
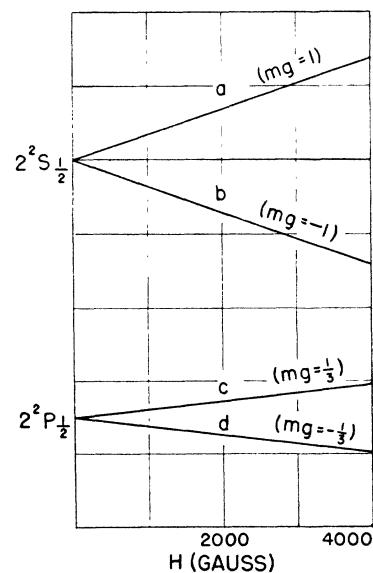
FIG. 3. Zeeman effect for the $2^2S_{\frac{1}{2}}$ and $2^2P_{\frac{1}{2}}$ states.
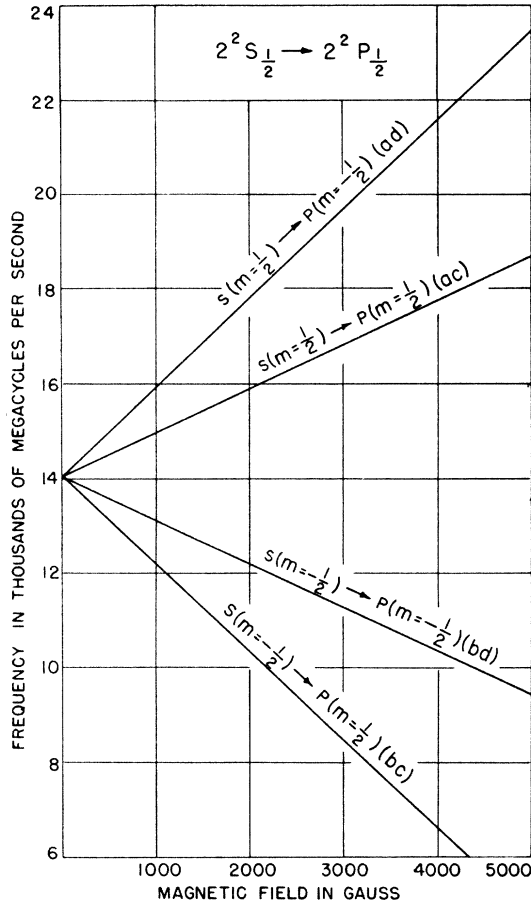
FIG. 4. Zeeman transition frequencies as a function of the magnetic field.

which becomes (see Appendix I)

$$\nu_r = \nu_0 + aH + bH^2, \tag{6}$$

where $b = 2.5 \times 10^{-6}$ mc/sec./gauss^2.

If the probability per second of an induced transition from $2^2S_{\frac{1}{2}}(m = +\frac{1}{2})$ to $2^2P_{\frac{1}{2}}(m = -\frac{1}{2})$ is μ, then[9]

$$\mu \propto 1/[(\nu - \nu_r)^2 + (A/4\pi)^2], \tag{7}$$

where ν is the frequency of the incident radiation, ν_r is the resonant frequency, and $A = 10^{10}$ sec.$^{-1}$ is the radiative half-width of the $2^2P_{\frac{1}{2}}$ state. Substituting Eq. (6)

TABLE II. Cross sections for excitation and ionization in helium.

Atomic cross sections[a] (in units of πa_0^2)	Ionic cross sections (in units of πa_0^2)
$\sigma(2^1S) = 0.49 \times 10^{-2}$	$\sigma^+(2^2S) = 0.37 \times 10^{-2}$
$\sigma(2^1P) = 6.9 \times 10^{-2}$	$\sum\limits_{n=2}^{\infty} \sigma^+(n^2P) = 2.8 \times 10^{-2}$
$\sigma(3^1P) = 2.1 \times 10^{-2}$	
$\sigma(4^1P) = 0.86 \times 10^{-2}$	
$\sigma(5^1P) = 0.46 \times 10^{-2}$	

[a] H. S. W. Massey and C. B. O. Mohr, Proc. Roy. Soc. **140A**, 613 (1933).

[9] See article by G. Wentzel in *Handbuch der Physik* (1933), second edition, 24/1, p. 757.

for ν_r, and H_0 for $(\nu - \nu_0)/a$, this becomes

$$\mu \propto 1/[(\nu - \nu_0 - aH - bH^2)^2 + (A/4\pi)^2] \tag{8}$$

or

$$\mu \propto 1/[(H_0 - H - bH^2/a)^2 + (\Gamma/2)^2], \tag{9}$$

where $\Gamma = A/2\pi a = 855$ gauss.

There are some possible corrections to (9) which must be considered. Use of the Bohr magneton in Eqs. (3) and (4) neglects effects due to the motion of the nucleus. The error introduced in Eq. (5) by using μ_0 is completely negligible, however, being less than 0.01 percent. Secondly, recent experimental results and theoretical considerations show that the gyromagnetic ratio of the electron spin is not 2, which was used to find Eq. (5), but $2 + \alpha/\pi$. Neglect of the term α/π introduces about 0.06 percent error in Eq. (5), which is again negligible.

For low r-f power, Eq. (9) gives the shape of the resonance obtained by varying H. The peak of the curve is at $H = H_1$, where $H_1 + bH_1^2/a = H_0$. The term bH^2/a is considerably smaller than H; at 4000 gauss, bH^2/a is about 20 gauss. Since this is the case, it can be shown that, for low r-f power, the half-width of the resonance is very nearly $\Gamma = 855$ gauss.

From the definition of H_0, we see that the zero magnetic field resonant frequency is

$$\nu_0 = \nu - aH_1 - bH_1^2, \tag{10}$$

where ν is the oscillator frequency and H_1 is the magnetic field at the resonance peak. This is the expression that was used to determine the shift of the $2^2S_{\frac{1}{2}}$ state above the $2^2P_{\frac{1}{2}}$ state, from the experimental curves.

4. DETECTION

The metastable ions are formed by the collisions of electrons with normal helium atoms. An electron energy greater than 65 ev is required, and electron energies of 150 or 200 ev were used. As mentioned before, we look for an increase in 41-ev photons when the metastable ions are quenched by the r-f induced transition to the $2^2P_{\frac{1}{2}}$ state. Unfortunately, the signal to background ratio is not very large. (The signal is that part of the detector current affected by the r-f. The background is the detector current when there is no r-f quenching.) This is a necessary result of the fact that the metastable state of the ion is just one of many states excited by collisions between electrons and helium atoms.

A. Theoretical Signal

The maximum signal, obtained when the r-f power is high enough to quench all the metastable ions formed, is directly proportional to the cross section for excitation of the metastable state of the ion in a collision between a normal helium atom and a 200-ev electron, and is given by

$$\begin{aligned} i_0 &= NIl(\omega/4\pi)\eta_{41}\sigma^+(2^2S) \\ &= K\eta_{41}\sigma^+(2^2S). \end{aligned} \tag{11}$$

In this expression N is the density of helium atoms, I is the bombarding electron current, l is the length of the electron beam from every point of which an unobstructed path can be drawn to the detector, ω is the solid angle subtended by the detector at the excitation region, η_{41} is the photoelectric efficiency of 41-ev photons, and $\sigma^+(2^2S)$ is the cross section for excitation to the metastable state of the ion.

In Appendix II, the value of $\sigma^+(2^2S)$ is estimated to be

$$\sigma^+(2^2S) = 0.37 \times 10^{-2} \pi a_0{}^2. \tag{12}$$

In order to obtain a quantitative estimate of i_0 we assume that η_{41} is of the order of 0.1. (See Section 4-C.) The values of l and $\omega/4\pi$ for the apparatus used are respectively 0.38 cm and 1.4×10^{-3}. Then, for an electron bombarding current of 0.2 ma and a pressure of 5×10^{-3} mm Hg, the expected value of i_0 is 6×10^{-14} ampere. If the background current were small, such a signal could be easily measured.

B. Sources of Background Current

There are three sources of background current to the detector: (a) Most of those atoms excited to the n^2P states of the ion decay to the ion ground state. The decay photons of energy 41 ev or greater produce photoelectric current at the detector. (b) Those atoms excited to the atomic metastable 2^1S_0 state cause background current by ejecting electrons from the detector plate.[10] (c) Most of the atoms excited to singlet n^1P_1 states of the atom decay to the ground state of the atom with the emission of photons of about 20-ev energy. Effects arising from the excitation of the atoms to the triplet states or to states with $L > 1$ are negligible since, at the electron energies used, such excitations are very much less probable than excitation to the singlet states with L equal to zero or one.

In order to estimate the relative contributions from these three processes, we need to know the cross sections for the n^2P states of the ion and for the 2^1S_0 metastable state and the n^1P_1 states of the atom. From Appendix II, where the cross sections in question are discussed, we have the results given in Table II, where a plus sign indicates that the cross section is for excitation to a state of the ion.

Since $\sigma(2^1P)$ is the largest cross section, it might be expected that most of the background current would be caused by the 20-ev radiation from the $2^1P_1 \rightarrow 1^1S_0$ transition. This is resonance radiation, however, and is highly absorbed in the gas between the excitation region and the detector. In Appendix III we compute the fraction, T_n, of photons arising from the transition $n^1P_1 \rightarrow 1^1S_0$ which reach the detector without being absorbed at least once in the gas at a pressure of 5×10^{-3} mm. For instance, only 0.08 percent of the photons from the $2^1P_1 \rightarrow 1^1S_0$ transition which are emitted in the direction of the detector reach it without

[10] R. Dorrestein, Physica 9, 433 and 447 (1942).
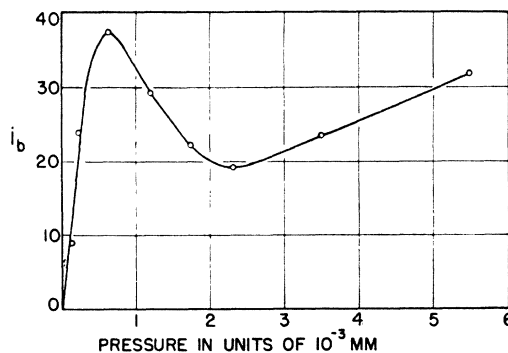
Fig. 5. Background current as a function of the pressure.

being absorbed. The absorption and re-emission of a photon does not necessarily mean that it is lost to the detector. An exact analysis of the situation is difficult, since one cannot define a mean free path for resonance radiation. It is likely, however, that a photon that strikes the walls of the apparatus is lost. This indicates that most of the photons reaching the detector do so without absorptions. We therefore define an effective cross section for excitation to the n^1P_1 states given by

$$\sigma^*(^1P) = \sum_{n=2}^{\infty} T_n \sigma(n^1P). \tag{13}$$

We shall assume, then, that the photoelectric current from $n^1P_1 \rightarrow 1^1S_0$ photons is $K \eta_{20} \sigma^*(^1P)$, where K is the proportionality factor given in Eq. (11) and η_{20} is the photoelectric efficiency of 20-ev photons. In Appendix III it is shown that $\sigma^*(^1P) = 0.95 \times 10^{-2} \pi a_0{}^2$.

The effect of the absorption of resonance radiation on the background current is shown in Fig. 5, where the experimental detector current is plotted as a function of the pressure. Assuming, as we have, that the current is due to (a) photo-electrons from photons of energy 41 ev or greater arising from the transitions $n^2P \rightarrow 1^2S_{\frac{1}{2}}$ of the ion, (b) electrons ejected by metastable atoms, and (c) photo-electrons from the 20-ev photons emitted in the transitions $n^1P_1 \rightarrow 1^1S_0$ of the atom, this curve is easily interpreted. At low pressures the detector current increases linearly with the pressure. In the vicinity of 4×10^{-4} mm there commences to be a significant amount of absorption of 20-ev photons. Since the cross sections for the lower n^1P_1 atomic levels are much larger than either

$$\sum_{n=2}^{\infty} \sigma^+(n^2P)$$

or $\sigma(2^1S)$, the signal actually decreases as the pressure is increased from 5×10^{-4} mm to 2.5×10^{-3} mm. At sufficiently high pressures, when the contributions from (a) and (b) become significant, the current increases again with pressure. (One would not expect any considerable absorption of 41 ev photons by either ions or atoms; the ion population is low, and the atomic ab-
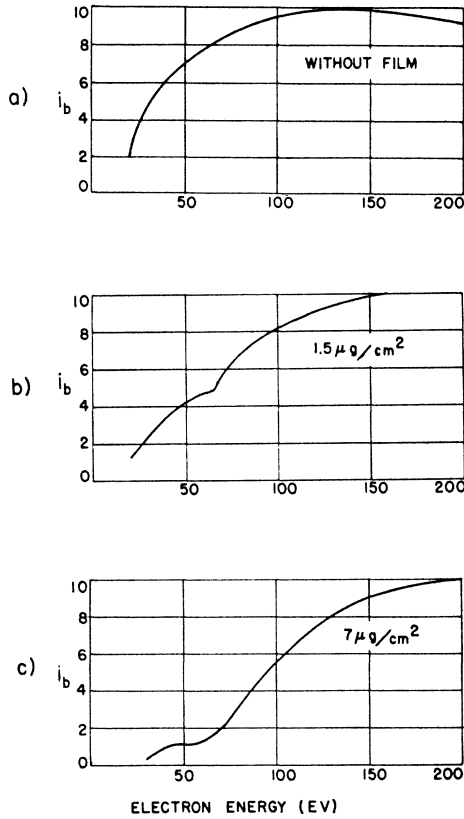
Fig. 6. Excitation curves showing the effect of the collodion film. The electron bombarding current for (a) was 3 μa, for (b) 100 μa, and for (c) 350 μa.

sorption cross section[11] is only about 3×10^{-18} cm^2. It is possible that deflecting collisions between the excitation region and the detector reduce the contribution from the metastable atoms.[10] We shall assume in what follows, however, that this is not important.)

For the background current we can now write

$$i_b = K\left[\eta_{41} \sum_{n=2}^{\infty} \sigma^+(n\,^2P) + \eta_{20}\sigma^*(^1P) + \eta_m\sigma(2\,^1S) \right], \quad (14)$$

where K is the proportionality factor given in Eq. (11), η_{41} and η_{20} are the photoelectric efficiencies of 41-ev and 20-ev photons, and η_m is the electron ejection efficiency of metastable atoms.

C. Theoretical Signal to Background Ratio

The maximum signal to background ratio is given by

$r = i_0/i_b$

$$= \eta_{41}\sigma^+(2^2S) \left/ \left[\eta_{41} \sum_{n=2}^{\infty} \sigma^+(n\,^2P) \right. \right.$$

$$\left. + \eta_{20}\sigma^*(^1P) + \eta_m\sigma(2\,^1S) \right]. \quad (15)$$

[11] S. Huang, Astrophys. J. 108, 354 (1948). We are indebted to Dr. Huang for informing us of his results prior to the publication of his paper.

We now need the relative values of η_{41}, η_{20}, and η_m. The detector plate was made of copper and was not outgassed. Dorrestein[10] found an efficiency of 0.4 for metastable helium atoms and a photoelectric efficiency of 0.08 for 20-ev photons on outgassed platinum. For the purposes of our rough estimate, we assume that Dorrestein's value of 5 for η_m/η_{20} holds in our case also. The only information available on the photoelectric efficiency of 41-ev photons is that of Kenty[12] who found that the photoelectric efficiencies of several metals were rising sharply with photon energy in the vicinity of 584A (20 ev). Since, however, one can draw no definite conclusions from this about the behavior of 41-ev photons, we shall assume that $\eta_{41} = \eta_{20}$. Thus

$$r = \sigma^+(2^2S) \left/ \left[\sum_{n=2}^{\infty} \sigma^+(n^2P) + \sigma^*(^1P) + 5\sigma(2^1S) \right] \right. . \quad (16)$$

Substituting our values for the cross sections we find that $r = 6 \times 10^{-2}$. It should have been possible, thus, to obtain a 6 percent increase in the detector current when the r-f power was turned on.

D. Experimental Signal to Background Ratio

With the apparatus as described in Section 2, a signal was obtained which was in good agreement with the estimated theoretical value. The maximum signal to background ratio observed, however, was 1.5 percent. The theoretical estimate made in the last section was apparently optimistic by a factor of 4, which is not surprising considering the assumptions that had to be made in deriving the various cross sections and efficiencies.

If the maximum signal to background ratio is 1.5 percent, less than half of this can be used in taking data for resonance curves. Only half of the metastable ions have magnetic quantum number $m = +\frac{1}{2}$, and only these are quenched in the transition between the Zeeman components $2^2S_{\frac{1}{2}}(m = +\frac{1}{2})$ and $2^2P_{\frac{1}{2}}(m = -\frac{1}{2})$. In order to obtain sharp resonances, well-isolated from
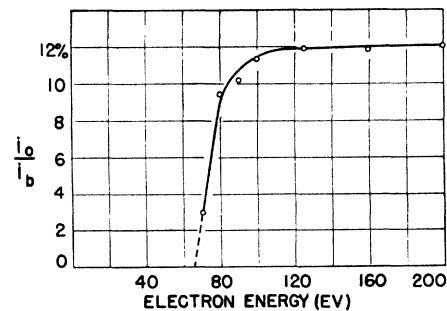
Fig. 7. R-f quenching as a function of the bombarding electron energy. The ordinate is the percent increase in the detector current when the r-f power was turned on. This curve was taken with a thick collodion film in the apparatus, and with a large amount of r-f power.

[12] C. Kenty, Phys. Rev. 44, 891 (1933).

FIG. 8. Cross section of
the wave guide in the ex-
citation region.

FIG. 9. Peak signal and resonance half-width as a function
of the r-f power.
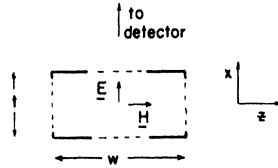
neighboring resonances, the r-f power is made lower than that required to quench all of the $2^2S_{\frac{1}{2}}(m=+\frac{1}{2})$ ions at the peak of the resonance.

Some very rough resonances were obtained, with peak quenching of about 0.3 percent. The data obtained were quite unsatisfactory, however. With a peak quenching of only 0.3 percent, one must hope to obtain good data on the wings of the resonance with less than 0.1 percent quenching. This means that variations in the background current must be held down to less than 0.05 percent, and this is difficult to accomplish.

E. Improvement of Signal to Background Ratio with Collodion Film

In order to improve this unfavorable signal to background ratio, a thin collodion film was placed in the apparatus at F (Fig. 2), between the excitation region and the detector. This would eliminate any contribution to the detector current from metastable atoms. In addition, the work by O'Bryan[13] on thin celluloid films indicated that collodion, similar in composition to cel-luloid, should have a higher absorption coefficient for 20-ev photons than for 41-ev photons.

The actual behavior of the collodion in eliminating contributions to the background current from meta-stable atoms and 20-ev photons is shown in Fig. 6. A rough excitation curve is shown in (a), giving the current as a function of the energy of the exciting electrons, with no collodion film in the apparatus. The current starts at 20 ev with the production of excited atomic levels. There is no observable contribution from the excitation of the ionic levels at 65 ev. A similar excitation curve with a thin collodion film, 1.5 $\mu g/cm^2$ (about 100A), in the apparatus is given in (b). Here for the first time effects due to the excitation of the ionic levels are observable. Presumably, in this case the current is due only to 20- and 41-ev photons, the film having cut out the metastable atoms. Finally, in (c), we see that with a thicker film, 7 $\mu g/cm^2$, the back-ground current from sources other than excited states of the ion has been reduced to about ten percent.

With a sufficiently thick film in the apparatus, the background current should be almost entirely due to 41-ev photons arising from the $n^2P\rightarrow1^2S_{\frac{1}{2}}$ transitions of the ion. Under these conditions, the signal to background ratio is

$$r'=\sigma^+(2^2S)\Big/\sum_{n=2}^{\infty}\sigma^+(n^2P). \qquad (17)$$

[13] H. M. O'Bryan, J. Opt. Soc. Am. **22**, 739 (1932).
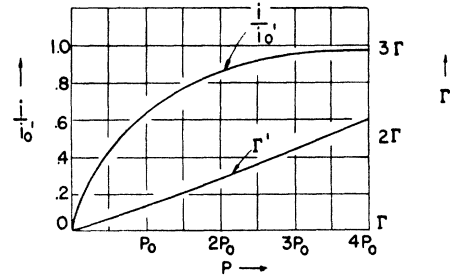
According to our estimates of these cross sections, the maximum signal to background ratio should be 13 percent. The experimental signal to background ratio was 12 percent, in good agreement with this theoretical estimate. (The signal to background ratio is increased slightly by working at lower pressures, which indicates that some of the metastable ions are lost by collisions at high pressures. We did not investigate this behavior very thoroughly. At pressures of 5×10^{-3} mm, however, less than half the metastable ions were lost. The reason for working at high pressures was simply to obtain a large enough signal to make random fluctuations in the galvanometer current insignificant. In Appendix IV, there is a discussion of the possibility of losing meta-stable ions due to Stark effect quenching. It is shown that, under the conditions of this experiment, this effect is negligible.)

Figure 7 shows the percentage increase in detector current with r-f quenching as a function of the energy of the bombarding electrons, when the r-f power is high and when there is a thick collodion film in the apparatus. For electron energies above 100 ev there is a 12 percent quenching signal. There is no indication of any quenching below 65 ev, the threshold for the production of metastable ions.

The resonance curves for the $2^2S_{\frac{1}{2}}(m=+\frac{1}{2})\rightarrow2^2P_{\frac{1}{2}}$ $(m=-\frac{1}{2})$ transitions were obtained with a peak r-f quenching of 4 or 5 percent.

5. RADIOFREQUENCY POWER REQUIRED

The probability per second of the induced transition $2^2S_{\frac{1}{2}}(m=+\frac{1}{2})\rightarrow2^2P_{\frac{1}{2}}(m=-\frac{1}{2})$ is[9]

$$\mu=\frac{2\pi S_0}{\hbar\omega}\frac{e^2}{\hbar c}\frac{A\omega}{(\omega-\omega_0)^2+(A/2)^2}|\mathbf{r}_{ad}\cdot\mathbf{E}|^2, \qquad (18)$$

where A is the width of the P state, ω_0 the resonant frequency and ω the frequency of the r-f, all in radians per second, S_0 is the incident power in ergs/cm^2 per second, $\mathbf{r}_{ad}$ is the vector whose components are the matrix elements for the transition, and $\mathbf{E}$ is a unit vector along the direction of polarization. In this case, with the wave guide transmitting radiation in the TE_{01} mode, $|\mathbf{r}_{ad}\cdot\mathbf{E}|=|x_{ad}|$ (see Fig. 8). At resonance we have

$$\mu=(8\pi e^2/\hbar^2c)S_0|x_{ad}|^2A^{-1}. \qquad (19)$$

Now $x_{ad} = (\sqrt{3}/2)a_0$. Using this and the values $A = 10^{10}$ sec.$^{-1}$ and P (in watts) $= \frac{1}{2}S_0 w \times l \times 10^{-7}$, where w and l are the dimensions of the guide, we obtain

$$\mu = 17 \times 10^6 P \text{ sec.}^{-1}. \qquad (20)$$

The photoelectric current produced at the detector when there is sufficient r-f power to quench all of the $2^2S_{\frac{1}{2}}(m = +\frac{1}{2})$ metastable ions that are formed in the wave guide is $i_0/2 = i_0'$ (see Eq. (11)). The photoelectric current for any value of the r-f power is then

$$i = i_0'(1 - e^{-\mu \tau_d}), \qquad (21)$$

where τ_d is the time spent by a metastable ion in a region in the wave guide from which there is an unobstructed path to the detector. There is a circular opening in the wave guide whose diameter is 0.38 cm, facing the detector, and τ_d will be equal roughly to this length divided by v, the velocity with which the ions diffuse out of the region.

There are two velocities which must be considered before calculating τ_d. The first of these is the thermal velocity of the ions. In a magnetic field, the ions will spiral about the flux lines. Thus, only the z-component of the velocity has to be considered. The average speed in the z-direction at 300°K is given by

$$\langle v_z^2 \rangle_{\text{Av}}^{\frac{1}{2}} = (kT/M)^{\frac{1}{2}} = 8 \times 10^4 \text{ cm/sec.} \qquad (22)$$

The average recoil velocity of the ions due to the electron collisions is harder to evaluate. The maximum recoil velocity occurs, however, when the incident electron is scattered through 180° and when the momentum of the electron knocked out of the atom is equal in direction and magnitude to that of the scattered electron. In this case

$$v = (m/M)[v_0 + (2v_0^2 - 4Q/M)^{\frac{1}{2}}], \qquad (23)$$

where m and v_0 are the mass and initial velocity of the bombarding electron, M is the mass of the atom (or
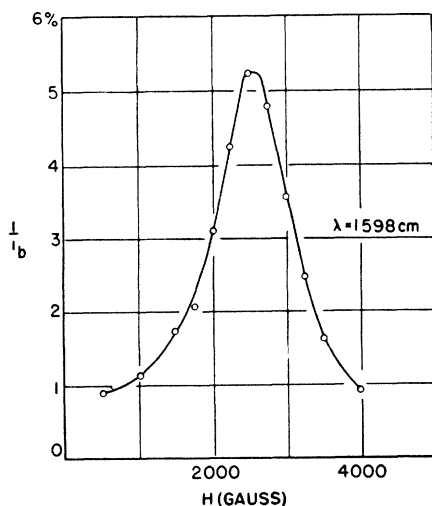
Fig. 10. Experimental resonance curve.

ion), and Q is the transition energy from the ground state of the atom to the excited state of the ion. In this case $Q(65 \text{ ev}) = 1.05 \times 10^{-10}$ erg and for a 200-ev incident electron $v_0 = 8.4 \times 10^8$ cm/sec. Substituting these values in Eq. (23), we find that the maximum recoil velocity is 2.5×10^5 cm/sec.

Since the recoil velocity distribution is not known, we do not know how to combine the recoil and thermal velocities to obtain an average value for the resultant. Instead, since the maximum recoil velocity is larger than the average thermal velocity, we shall use it to calculate τ_d. The average recoil velocity is probably much smaller than 2.5×10^5 cm/sec. Therefore, we should in this way find a value for the order of magnitude of the power required to obtain a given photoelectric current which is higher than the actual power requirement.

Using $v = 2.5 \times 10^5$ cm/sec., we find that $\tau_d = 1.5 \times 10^{-6}$ sec. The condition for $i = 0.63i_0'$ is that $\mu \tau_d$ be equal to unity. Thus, in order to quench 63 percent of the $(m = +\frac{1}{2})$ metastable ions, we need about 40 milliwatts of r-f power.

For $\mu \tau_d \ll 1$, we have $i = i_0' \mu \tau_d$. In this case the shape of a resonance obtained by varying the magnetic field is given by Eq. (9). With low r-f power, the half-width of the resonance should thus be about 855 gauss. For higher r-f power, the resonance is broadened. In Fig. 9 the resonance value of i/i_0' and the half-width, Γ', as determined by Eqs. (20), (21), and (9), are plotted as a function of the power. The power is in units of P_0, the power required to quench 63 percent of the metastable $2^2S_{\frac{1}{2}}(m = +\frac{1}{2})$ ions, and the half-widths are given in units of Γ, where $\Gamma = 855$ gauss.

6. DETAILED DESCRIPTION OF THE APPARATUS

With the pole piece arrangement used, the electromagnet gave fields up to 4000 gauss. The magnet current, which at 4000 gauss was 1.5 amperes, was supplied by a rectifying unit consisting of a voltage doubling transformer, a selenium rectifier and two filter sections. The 115-volt a.c. input to the rectifier was stabilized with a Sola transformer. The field was calibrated by means of a rotating flip coil which had been previously calibrated in a standard field. An upper limit on the error in the magnetic field calibration is 0.5 percent. The uniformity of the field was investigated by means of a flip coil and a General Electric flux meter. In the wave guide region the field was uniform to better than 0.5 percent.

The source of radiofrequency power was a continuous wave magnetron. The meaningful results of the experiment were obtained using cw magnetrons in the 1.6-cm wave-length range. These tubes[14] were made for the experiment in the Columbia Radiation Laboratory under the direction of M. J. Bernstein, to whom we are indebted for keeping us supplied.

A wave guide was used to transmit the r-f radiation

[14] Columbia Radiation Laboratory Report (September 30, 1948), p. 8.

from the magnetron to the excitation region. In the excitation region, the guide dimensions were 0.180 in. by 0.360 in. Circular holes 0.150 in. in diameter were cut in the walls of the guide to allow the electron beam to pass through the guide and to allow the photons passage to the detector. At $\lambda=1.60$ cm, the guide wave-length is 1.31 in., which is long compared to the diameter of the holes, so the holes should not disturb the transmission of the r-f power in the TE_{01} mode to any considerable extent. Connections were made from the vacuum regions of the guide to the non-vacuum regions through mica windows. The r-f power was monitored by the crystal current from a standing wave machine which was situated between the magnetron and the excitation region. Beyond the excitation region the r-f fed into a TE_{01n} two centimeter cylindrical wave meter,[15] by means of which the wave-length could be determined to about 0.1 percent. On the other side of the wave meter the r-f fed into a matched load.

The current heating the filament of the electron gun was supplied by storage batteries, which were charged continuously through a selenium rectifier. The electrical connections in the filament circuit were made with great care, since the detector current was extremely sensitive to variations in this filament current, being directly proportional to the filament emission. The current to the filament was varied by means of an Ohmite resistor in an oil bath.

Two grades of helium were used, the welding grade, 99.95 percent pure, and the XX grade, 99.99 percent pure, obtained from the Ohio Chemical and Manufacturing Company.

Aside from the mica windows in the wave guide, all vacuum seals were either soldered or brazed, if permanent, or waxed with Apiezon W, if temporary. The apparatus was pumped continuously, with a forepump and a three-stage oil diffusion pump, and could be pumped down to a pressure of 2×10^{-6} mm in 3 or 4 hours. Helium was admitted to the apparatus directly from the tank through a leak which was made by inserting a short length of 0.010-in. tungsten wire in a Pyrex capillary tube of about 0.030-in. bore and making a leaky glass-to-metal seal. The helium pressure in the apparatus was read by means of an ionization gauge, using the calibration data supplied by Distillation Products, Inc. for the VG-1A gauge, and correcting for the distance from the ionization gauge to the excitation region.

For the measurement of the detector current, a Victoreen VX 41 electrometer tube was used in a Penick[16] d.c. amplifier circuit. The Penick circuit is designed to operate in a balanced condition such that the galvanometer current is independent of small fluctuations in the tube filament current. Although for most of the work in this experiment the circuit was not so

balanced, the amplifier gave entirely satisfactory results. All electrode voltages were supplied by two 6-volt "A" batteries. The leads to the electrometer tube were shielded electrically, and the tube itself was shielded magnetically by being placed in a cylinder of soft iron. The lead from the apparatus to the control grid of the tube was at all points insulated from other metal parts by at least a quarter of an inch of air. No attempt was made to mount the tube in vacuum, or to use drying agents in its vicinity. In spite of this, the galvanometer current was very steady. There was no noticeable change in the sensitivity of the whole detection system in a period of more than a year. The response of the amplifier was linear up to a control grid voltage of about 0.1 volt. Above this voltage, the slope of the response curve increased with control grid voltage.

The galvanometer used was a Leeds and Northrup Type R. The sensitivity of amplifier and galvanometer was 1.2×10^{-5} volt/mm. A grid resistor of 10^{11} ohms was used, giving a current sensitivity of 1.2×10^{-16} ampere/mm. With no signal coming to the detector, galvanometer and amplifier unsteadiness amounted to random fluctuations of about 1 mm, with occasional 2- or 3-mm fluctuations.

The collodion for the thin films was diluted to the required strength with amyl acetate. With an eye-dropper, a drop was placed on the surface of clean distilled water. When the interference fringes disappeared from the film that formed on the water, it was picked up on a copper frame which had been suspended under the water surface. This was done in such a way that a double film covered the frame. After a short drying time, the frame was placed in the apparatus. The process of making the films was quite simple, except in the case of very thin films which displayed many fine cracks if they were allowed to harden too much on the water before being raised on the frame. The thickness of the films was determined only very roughly by weighing several drops of the diluted collodion on an analytical balance and dividing the weight per drop by the area over which the drop spread. We are very much indebted to Dr. C. S. Wu for information about mounting collodion films.

7. DISCUSSION OF THE DATA

In obtaining resonances, several fixed r-f frequencies were used, resulting in quite widely differing peak mag-

TABLE III. Level shift of $2^2S_{\frac{1}{2}}-2^2P_{\frac{1}{2}}$ in He$^+$.

ΔW_2 (in mc/sec.)	
14,070	14,050
14,010	14,050
14,010	14,040
14,030	14,030
13,980	14,050
13,970	13,980
	Average = 14,020
	(Statistical error = ±10)

[15] Columbia Radiation Laboratory Report (September 30, 1948), p. 11.
[16] D. B. Penick, Rev. Sci. Inst. 6, 115 (1935).

netic fields. The slope of the line obtained by plotting the frequency as a function of the peak magnetic field was equal to 1.87 mc/sec. per gauss (see Eq. (5)), showing that the resonances did indeed belong to the (ad) $2^2S_{\frac{1}{2}}(m=+\frac{1}{2})\to2^2P_{\frac{1}{2}}(m=-\frac{1}{2})$ transition.

The most accurate data were taken with r-f wave-lengths between 1.52 cm and 1.61 cm, corresponding to peak magnetic fields between 3050 gauss and 2450 gauss. Figure 10 shows a typical resonance curve.

Before applying Eq. (10) to the resonance curves, in order to obtain the zero magnetic field level shift, the influence of two neighboring Zeeman transitions must be considered. First, there is the (ac) $2^2S_{\frac{1}{2}}(m=+\frac{1}{2})\to$ $2^2P_{\frac{1}{2}}(m=+\frac{1}{2})$ transition, also originating in the $m=+\frac{1}{2}$ component of the $2^2S_{\frac{1}{2}}$ state (see Fig. 4). The only matrix element of the vector r which does not vanish for the (ac) transition is z_{ac} where z is in the direction of the magnetic field. Since the electric field is along x (see Fig. 8 and Eq. (18)), this transition is not induced by the r-f. Secondly, there is the (bc) $2^2S_{\frac{1}{2}}(m=-\frac{1}{2})\to$ $2^2P_{\frac{1}{2}}(m=+\frac{1}{2})$ transition, originating in the $m=-\frac{1}{2}$ component of the $2^2S_{\frac{1}{2}}$ state. For r-f frequencies above 14,000 mc/sec., the peak of this transition occurs at "negative" magnetic fields. Since $x_{bc}=x_{ad}$, this transition can be induced if there is enough r-f power to compensate for the large off-resonance term which appears in the denominator of Eq. (18). It was in this way that we were able to quench all of the metastable ions with high r-f power and see a 12 percent signal to background ratio instead of the 6 percent maximum which would have been observed if only those metastable ions with $m=+\frac{1}{2}$ had been quenched. The (bc) transition spoils the symmetry of the (ad) resonance in the wings by raising the low magnetic field wing above the high magnetic field wing (see Fig. 10). It can be shown, however, that with sufficient power to obtain about 5 percent quenching for the (ad) transition, or a signal due to quenching five-sixths of the $m=+\frac{1}{2}$ metastable ions, the shift in the (ad) resonance peak magnetic field due to the influence of the (bc) transition amounts to only about 2 gauss, if the peak is in the vicinity of 2500 gauss. This corresponds to about 4 mc/sec., which can be neglected for this experiment. Therefore, no corrections for neighboring transitions are necessary before applying Eq. (10).

The value of the peak magnetic field, H_1, to be used in Eq. (10) was found graphically for each resonance.

The narrowest resonance curve that we observed had a half-width of about 1150 gauss. This was with a peak quenching of 2.8 percent. Consulting Fig. 9, it is seen that for $i/i_0'=2.8/6=0.47$, the width should be 1.2Γ, or about 1020 gauss. We did not investigate the widths for very low r-f powers since, with the collodion film in the apparatus, a higher detector sensitivity would have been required to do so.

8. RESULTS

Applying Eq. (10) to twelve resonances, the values shown in Table III were obtained for the $2^2S_{\frac{1}{2}}-2^2P_{\frac{1}{2}}$ level shift.

There are three possible sources of error: (a) Accidental errors, made in locating the resonance peak magnetic field, which are evidenced by the fluctuations in the values in Table III, (b) error in the calibration of the wave meter used to measure the r-f wave-length, and (c) error in the calibration of the magnetic field. We take ±100 mc/sec. for the maximum total error introduced by the above.

Our experimental value for the $2^2S_{\frac{1}{2}}-2^2P_{\frac{1}{2}}$ level shift in ionized helium is thus

$$\Delta W_2=14{,}020\pm100 \text{ mc/sec.} \tag{24}$$

The average value is about 1.4 percent higher than the present theoretical value of 13,820 mc/sec. In addition, both the theoretical result and our experimental value are larger than the last two values in Table I.

It should be possible to obtain a more precise value for the level shift for ionized helium than for hydrogen, since, in the former case, the complicating factor of hyperfine structure is missing. The work reported here is of an exploratory nature. A new apparatus is being built in this laboratory for a more accurate measurement of the level shift in ionized helium.

APPENDIX I. CORRECTION TO EQ. (4) FOR PASCHEN—BACK EFFECT

The two components of the $2^2S_{\frac{1}{2}}$ state experience only a linear Zeeman effect. Therefore we need only the correction to Eq. (3) for the $m=-\frac{1}{2}$ component of the $2^2P_{\frac{1}{2}}$ state.

Let E_+ and E_- be the energies of the $2^2P_{3/2}$ and $2^2P_{\frac{1}{2}}$ states in the absence of a magnetic field. Then it can be shown[17] that the energy of the $2^2P_{\frac{1}{2}}(m=-\frac{1}{2})$ state for a magnetic field H is

$$E=\tfrac{1}{2}(E_++E_-)+\mu_0Hm-\tfrac{1}{2}[(E_+-E_-)^2 \\ +(4/3)\mu_0Hm(E_+-E_-)+(\mu_0H)^2]^{\frac{1}{2}}. \tag{25}$$

For ionized helium, the zero-field energy difference between the $2^2P_{3/2}$ and $2^2P_{\frac{1}{2}}$ states is, in frequency units,

$$(E_+-E_-)/h=175\times10^3 \text{ mc/sec.} \tag{26}$$

At 4000 gauss, the highest magnetic field used, the magnetic energy, also in frequency units, is $\mu_0H/h=5.6\times10^3$ mc/sec.

Since $(E_+-E_-)\gg\mu_0H$ for all magnetic fields used, we may expand the square root in Eq. (25), keeping only linear and quadratic terms in H:

$$E=E_-+\tfrac{2}{3}\mu_0Hm-2\mu_0^2H^2/9(E_+-E_-). \tag{27}$$

Thus, the correction to Eq. (3) for the $2^2P_{\frac{1}{2}}(m=-\frac{1}{2})$ state is $-bH^2$, where $b=2\mu_0^2/9h(E_+-E_-)=2.5\times10^{-6}$ mc/sec./gauss^2. Equation (4) then becomes Eq. (6) of the text

$$\nu_r=\nu_0+aH+bH^2.$$

For $H=2500$ gauss, $bH^2=16$ mc/sec.

APPENDIX II. EXCITATION CROSS SECTIONS

We are interested in the cross sections for the production of certain excited levels of helium by collisions between 200-ev

[17] See article by H. A. Bethe in *Handbuch der Physik* (1933), 24/1, second edition, p. 397.

electrons and normal helium atoms. The cross sections in question are those for the $2^2S_{\frac{1}{2}}$ (metastable) and n^2P states of the ion and for the 2^1S_0 (metastable) and n^1P_1 states of the atom.

Considering the atomic levels first, cross sections for the 2^1S_0 metastable state and for the first four n^1P_1 states ($n=2$ to $n=5$) were calculated by Massey and Mohr. Their results are given in Table II. Massey and Mohr's values for the $\sigma(n^1P)$ are very nearly equal to k/n^3 where $k=0.57\pi a_0{}^3$. When we have occasion to consider cross sections for excitation to the n^1P_1 states with $n>5$, we shall therefore use

$$\sigma(n^1P) = 0.57\pi a_0{}^2/n^3 \quad (n>5). \tag{28}$$

As far as we know, there is no work reported in the literature on excitation cross sections for the ionic levels. It is possible, however, to obtain rough estimates for these cross sections quite easily. Consider first $\sigma^+(2^2S)$, the cross section for excitation to the metastable $2^2S_{\frac{1}{2}}$ state of the ion. Originally the helium atom is in a state which can be approximated by the product of two hydrogen ground state wave functions with nuclear charge 1.69:

$$\psi_0 = \psi_{10}(1.69, \mathbf{r}_1)\psi_{10}(1.69, \mathbf{r}_2), \tag{29}$$

where $\psi_{nl}(Z, \mathbf{r})$ is a hydrogen wave function for an electron whose position vector is $\mathbf{r}$, in the field of a nucleus with charge Z. If, in a collision with an electron, the primary process is the excitation of electron 1 into the continuum, the second electron suddenly finds itself bound to a nucleus of charge 2, instead of effective charge 1.69, and is therefore no longer in a definite quantum state. To find the probability that the electron is left in the $2^2S_{\frac{1}{2}}$ state we use the "sudden" approximation,[18] in which the initial wave function of the second electron is expanded in terms of the eigenfunctions of the second electron in the new force field:

$$\psi_{10}(1.69, \mathbf{r}_2) = \Sigma a_{nl}\psi_{nl}(2, \mathbf{r}_2). \tag{30}$$

Then,

$$\sigma^+(2^2S) = \sigma^+|a_{20}|^2 = \sigma^+\left|\int \psi_{20}{}^*(2, \mathbf{r}_2)\psi_{10}(1.69, \mathbf{r}_2)d\tau_2\right|^2, \tag{31}$$

where σ^+ is the cross section for ionization. This yields

$$\sigma^+(2^2S) = 0.01\sigma^+. \tag{32}$$

Using Massey and Mohr's value of $0.37\pi a_0{}^2$ for σ^+, we find the result of Eq. (12) of the text.

The validity of the use of the sudden approximation is open to some question, since it assumes that the initial process that changes the Hamiltonian of the second electron, namely the excitation of the first electron to a state in the continuum, happens in a "short" time. We can show, however, that the use of the sudden approximation does yield predictions for two other similar double excitation processes which agree within a factor of two with results obtained by different methods.

Consider first the double ionization of the helium atom. Bleakney and Smith[19] found by mass spectrographic measurements that 0.5 percent of the ions formed at 200-ev bombarding electron energy were doubly charged. The sudden approximation treatment of this problem yields

$$\sigma^{++} = \sigma^+ \sum_{\text{continuum}} \left|\int \psi_c{}^*(2, \mathbf{r}_2)\psi_{10}(1.69, \mathbf{r}_2)d\tau_2\right|^2. \tag{33}$$

Since the $\psi(2, \mathbf{r}_2)$ form a complete set, this becomes

$$\sigma^{++} = \sigma^+\left[1 - \Sigma_n\left|\int \psi_{n0}{}^*(2, \mathbf{r}_2)\psi_{10}(1.69, \mathbf{r}_2)d\tau_2\right|^2\right]$$

$$= \sigma^+[1 - \Sigma_n|b_n|^2]. \tag{34}$$

Only the first few terms of the sum are significant. It can be

shown that $b_1 = 0.989$, $b_2 = -0.104$, and $b_3 = -0.038$. Thus

$$1 - \Sigma_n|b_n|^2 = 1 - 0.978 - 0.011 = 0.011. \tag{35}$$

The sudden approximation yields the result that 1.1 percent of the ions should be doubly ionized, which agrees well with Bleakney and Smith's value of 0.5 percent.

Next consider the double excitation of the helium atom to the state $(2s4p)^1P$. The cross section for this process was calculated by Massey and Mohr[20] using the Born approximation. The sudden approximation treatment assumes a primary excitation of one electron to a $4p$ state, the cross section for this process being very nearly $\sigma(4^1P)$. In the final state, the s-electron will see a charge on the nucleus which is close to 2. Using the sudden approximation, we therefore obtain

$$\sigma(2s4p) = \sigma(4^1P)\left|\int \psi_{20}{}^*(2, \mathbf{r}_2)\psi_{10}(1.69, \mathbf{r}_2)d\tau_2\right|^2$$

$$= 0.01\sigma(4^1P). \tag{36}$$

Massey and Mohr's values for $\sigma(2s4p)$ and $\sigma(4^1P)$ are $0.45\times10^{-4}\pi a_0{}^2$ and $0.86\times10^{-2}\pi a_0{}^2$. The ratio of these two cross sections 0.52×10^{-2} is in sufficiently good agreement with the above value of 0.01.

Although the sudden approximation is apparently applicable to the calculation of such cross sections as $\sigma^+(2^2S)$, σ^{++}, and $\sigma(2s4p)$, it is not clearly applicable to the calculation of the excitation cross sections for the low n^2P states of the ion. Consider, for example, $\sigma^+(2^2P)$. To calculate this by the sudden approximation, we would take as the primary process the excitation of one electron to a $2p$-state. As compared with the above cases for which the primary excitation is to a continuum or high principal quantum number p-state, one would now expect more interaction between the two atomic electrons during the excitation process, and therefore less validity for the sudden approximation procedure. In addition there is the practical objection that the presence of the first electron in the $2p$-state makes it difficult to find good approximations to the eigenfunctions of the second electron in the new potential field.

Since a treatment of the problem by more exact methods than the sudden approximation becomes very involved, we find a rough estimate of $\sigma^+(2^2P)$ in the following way. Massey and Mohr[20] calculated the double excitation cross sections $\sigma(2s3p)$ and $\sigma(3s2p)$ for helium, and found that

$$\frac{\sigma(2s3p)}{\sigma(3s2p)} = \frac{0.68\times10^{-4}\pi a_0{}^2}{5.3\times10^{-4}\pi a_0{}^2} = 0.13. \tag{37}$$

Our rough estimate is obtained by assuming that

$$\frac{\sigma^+(2^2S)}{\sigma^+(2^2P)} = \frac{\sum\limits_{\text{continuum}} \sigma(2s\infty p)}{\sum\limits_{\text{continuum}} \sigma(\infty s2p)} \cong \frac{\sigma(2s3p)}{\sigma(3s2p)} \cong 0.13. \tag{38}$$

With Eq. (12) this yields

$$\sigma^+(2^2P) = 2.8\times10^{-2}\pi a_0{}^2. \tag{39}$$

We assume that the total cross section for excitation to the n^2P states of the ion with $n>2$ is much less than $\sigma^+(2^2P)$, and therefore write

$$\sum_{n=2}^{\infty} \sigma^+(n^2P) = 2.8\times10^{-2}\pi a_0{}^2. \tag{40}$$

(One cannot, by a similar argument, neglect the excitation of the atomic n^1P_1 states with $n>2$. It is shown in Appendix III that the absorption of the resonance radiation from the $n^1P_1 \to 1^1S_0$ transitions increases the relative importance of excitation to states with high n.)

[18] F. Bloch, Phys. Rev. 48, 187 (1935) used the sudden approximation to treat an analogous problem in the theory of x-ray satellites.

[19] W. Bleakney, Phys. Rev. 43, 378 (1933). W. Bleakney and L. G. Smith, Phys. Rev. 49, 402 (1936).

[20] H. S. W. Massey and C. B. O. Mohr, Proc. Camb. Phil. Soc. 31, 604 (1935).

TABLE IV. Probability (T_n) that photons reach the detector.

Transition	k_0	T_n
$2^1P_1 \rightarrow 1^1S_0$	50 cm^{-1}	0.08×10^{-2}
$3^1P_1 \rightarrow 1^1S_0$	12 cm^{-1}	0.38×10^{-2}
$4^1P_1 \rightarrow 1^1S_0$	4.5 cm^{-1}	1.2×10^{-2}
$5^1P_1 \rightarrow 1^1S_0$	2.3 cm^{-1}	2.5×10^{-2}

APPENDIX III. ABSORPTION OF THE RESONANCE RADIATION ARISING FROM THE $n^1P_1 - 1^1S_0$ TRANSITIONS IN HELIUM

In a paper on the imprisonment of resonance radiation, Holstein[21] derived the following expression for the probability that a photon emitted in a transition from an excited state of principal quantum number n to the ground state of the atom traverse a distance ρ without being absorbed

$$T_n(\rho) = (k_0\rho)^{-1}(\pi \log k_0\rho)^{-\frac{1}{2}}. \tag{41}$$

In this expression k_0 is determined by

$$k_0 = \lambda_n^3 N g_n / 8\pi^{\frac{1}{2}} g_1 v_0 \tau_n, \tag{42}$$

where λ_n is the resonance wave-length of the radiation, N is the number of absorbing atoms per cm^3, g_n and g_1 are the statistical weights of the two states, $v_0 = (2kT/M)^{\frac{1}{2}}$, and τ_n is the lifetime of the excited state.

Equation (41) was developed on the basis of a Doppler spectral distribution, and holds only for values of $k_0\rho$ large compared to unity. Before using Eq. (41) for photons from the $n^1P_1 \rightarrow 1^1S_0$ transitions of helium, we must first show that the spectral distribution of each of the lines arising from these transitions is essentially a Doppler distribution.

We shall first consider the line $2^1P_1 \rightarrow 1^1S_0$. The natural width of this line is $A_2/2\pi$, where

$$A_2 = (64\pi^4 e^2 \nu_2^3 / 3hc^3)(|x|^2 + |y|^2 + |z|^2). \tag{43}$$

In this expression, x is given by

$$x = \int \psi_1^*(\mathbf{r}_1, \mathbf{r}_2)(x_1 + x_2)\psi_2(\mathbf{r}_1, \mathbf{r}_2)d\tau_1 d\tau_2. \tag{44}$$

Vinti[22] has calculated these matrix elements for the first few excited singlet P states. For the $2^1P_1 \rightarrow 1^1S_0$ transition, he obtained

$$|x|^2 + |y|^2 + |z|^2 = 0.224\pi a_0^2. \tag{45}$$

Substituting this, and the value $\nu_2 = 5.14 \times 10^{15}$ sec.$^{-1}$ (corresponding to a wave-length of 584A), we have

$$A_2 = 0.23 \times 10^{10} \text{ sec.}^{-1}. \tag{46}$$

Thus, the natural half-width of the resonance line is

$$\Delta\nu_N = A_2/2\pi = 0.36 \times 10^9 \text{ mc/sec.} \tag{47}$$

For a thermal velocity distribution of the normal and excited atoms, the Doppler width is given by

$$\Delta\nu_D = 2(2\ln 2)^{\frac{1}{2}}(kT/M)^{\frac{1}{2}}\nu_2/c. \tag{48}$$

One might expect that the excited atoms would not have a thermal velocity distribution because of the recoil velocity given them in the excitation collision with an electron. The great majority of the excited atoms, however, result from collisions in which the electron is scattered through less than 20 degrees (see Table II). For these collisions, the recoil energy of the atom is less than 0.003 ev, which is well below thermal energies. We shall, therefore, assume a thermal velocity distribution corresponding to a temperature of 300°K. We then find

$$\Delta\nu_D = 3.1 \times 10^4 \text{ mc/sec.} \tag{49}$$

Since the Doppler width is much larger than the natural width, the spectral distribution can be taken as a Doppler distribution, and if $k_0\rho$ is large, Eq. (41) can be applied. For the $n^1P_1 \rightarrow 1^1S_0$ lines, the ratio of $\Delta\nu_D$ to $\Delta\nu_N$ increases with n, so that the above statement holds for all n.

Using $g_n = 3$, $g_1 = 1$, $N = 1.8 \times 10^{14}$ corresponding to a pressure of 5×10^{-3} mm, and Vinti's values for the lifetimes of the excited states $\tau_n = 1/An$, we find the values given in Table IV for the probability T_n that photons from the $n^1P_1 \rightarrow 1^1S_0$ transition emitted in the direction of the detector will reach it without being absorbed. Since the detector plate is 6 cm from the excitation region, we have taken $T_n = T_n(6)$.

We define the total effective cross section for excitation to any of the n^1P_1 states by Eq. (13) of the text. The first four terms of this sum are known. Since T_n is 0.025 for $n = 5$, and is rapidly increasing, we approximate the contribution from terms with $n > 5$ by setting T_n equal to unity. We can then use Eq. (28) to evaluate

$$\sum_{n=2}^{\infty} \sigma(n^1P).$$

In this way, we find that

$$\sigma^*(^1P) = 0.95 \times 10^{-2}\pi a_0^2. \tag{50}$$

APPENDIX IV. STARK EFFECT QUENCHING OF METASTABLE IONS

Bethe[23] has developed the theory of the Stark effect mixing of the metastable $2^2S_{\frac{1}{2}}$ and the $2^2P_{\frac{1}{2}}$ states of a hydrogen-like atom for the case that these states are degenerate. In the non-degenerate case, let $h\nu_r$ be the energy difference between the two states. Then it can be shown[24] that the lifetime of the metastable state, as shortened by the Stark effect mixing, is given by

$$\tau_{2s} = \tau[\nu_r^2 + (A/4\pi)^2] / |V/h|^2, \tag{51}$$

where V is the matrix element of the perturbation energy, $H' = +e\mathbf{E} \cdot \mathbf{r}$, and $\tau = 1/A$ is the lifetime of the $2^2P_{\frac{1}{2}}$ state.

We shall consider the lifetime of the $2^2S_{\frac{1}{2}}(m = +\frac{1}{2})$ state of the ion for zero magnetic field. This will give a minimum lifetime since a magnetic field increases ν_r. Assuming that $\mathbf{E}$ is in the x direction (see Fig. 8), $V = +eEx = \sqrt{3}/2eEa_0$. For E in volts/cm,

$$|V/h| = 1.1 \text{ mc/sec.} \tag{52}$$

For ionized helium, $A = 10^4$ mc/sec., and in the absence of a magnetic field $\nu_r = 1.4 \times 10^4$ mc/sec. Equation (51) now yields

$$\begin{aligned}\tau_{2s} &= (1.6 \times 10^8/E^2)\tau \\ &= 1.6 \times 10^{-2}E^{-2} \text{ sec.}\end{aligned} \tag{53}$$

There will be no appreciable loss of metastable ions by Stark effect quenching if the $2^2S_{\frac{1}{2}}$ lifetime is long compared to the ion diffusion time τ_d. Therefore, the condition which must be satisfied is

$$\tau_d/\tau_{2s} \ll 1. \tag{54}$$

If for τ_d we use the value 1.5×10^{-6} sec. given in Section V, the requirement for small Stark quenching is found to be

$$E \ll 100 \text{ volt/cm.} \tag{55}$$

Since the stray electric fields in the apparatus due to space charge or other sources were considerably less than 100 volt/cm, the Stark effect quenching was negligible.

It is interesting to note that according to Eq. (51) the Stark effect lifetime of the He$^+$ metastable state is 42 times as large as that of hydrogen in the same perturbing electric field.

[21] T. Holstein, Phys. Rev. 72, 1212 (1947).
[22] J. P. Vinti, Phys. Rev. 42, 632 (1932).

[23] H. A. Bethe, reference 17, p. 454.
[24] W. E. Lamb, Jr. and R. C. Retherford (to be published).